Int. J. Dev. Biol. 61: 389-395 (2017)
doi: 10.1387/ijdb.160461sg

THE INTERNATIONAL JOURNAL OF DEVELOPMENTAL BIOLOGY
www.intjdevbiol.com

Identification and characterization of the autophagy-related genes *Atg12* and *Atg5* in hydra

NISHIKANT S. DIXIT, BHUPENDRA V. SHRAVAGE* and SURENDRA GHASKADBI*

Developmental Biology Group, MACS-Agharkar Research Institute, Pune, India

ABSTRACT Autophagy is an evolutionarily conserved process in eukaryotic cells that is involved in the degradation of cytoplasmic contents including organelles via the lysosome. Hydra is an early metazoan which exhibits simple tissue grade organization, a primitive nervous system, and is one of the classical non-bilaterian models extensively used in evo-devo research. Here, we describe the characterization of two core autophagy genes, *Atg12* and *Atg5*, from hydra. *In silico* analyses including sequence similarity, domain analysis, and phylogenetic analysis demonstrate the conservation of these genes across eukaryotes. The predicted 3D structure of hydra Atg12 showed very little variance when compared to human Atg12 and yeast Atg12, whereas the hydra Atg5 predicted 3D structure was found to be variable, when compared with its human and yeast homologs. Strikingly, whole mount *in situ* hybridization showed high expression of *Atg12* transcripts specifically in nematoblasts, whereas *Atg5* transcripts were found to be expressed strongly in budding region and growing buds. This study may provide a framework to understand the evolution of autophagy networks in higher eukaryotes.

KEY WORDS: *autophagy, hydra, Atg12, Atg5*

Introduction

Autophagy is a lysosome mediated process found in all eukaryotic organisms, and involves degradation of old organelles, toxic waste and misfolded proteins. It is a multistep process regulated by autophagy (Atg) specific proteins that involves formation of double membraned vesicles called autophagosomes. Autophagy is broadly classified into three types, viz. chaperone-mediated autophagy (CMA), microautophagy and macroautophagy (termed as autophagy henceforth) based on the proteins involved in the process and presence or absence of autophagosomes within the cytosol. The genes encoding these proteins were first discovered through multiple genetic screens in *Saccharomyces cerevisiae* (Tsukada and Ohsumi, 1993). Briefly, autophagy is initiated by Atg1 complex and the Vps34 complex which induce the formation of an isolation membrane which later expands to form the autophagosome. Autophagosome formation and completion requires two ubiquitin-like conjugation systems called the Atg12 and the Atg8 conjugation systems (Ohsumi and Mizushima, 2004). Atg12 is conjugated to Atg5 with the help of ubiquitin-activating E1-like enzyme Atg7 and, the ubiquitin-activating E2-like enzyme Atg10. The Atg12-Atg5 conjugate interacts with Atg16 to form the Atg12-Atg5-Atg16 complex. This complex is localized to the autophagosome membrane and catalyzes the lipidation of Atg8. Atg12-Atg5-Atg16 complex is detached from the autophagosome at a later stage (Otomo *et al.*, 2013).

Atg12 and Atg5 have been demonstrated to have crucial functions. For instance, Atg5-/- mice survive until birth but die within a few hours at the neonatal stage (Kuma *et al.*, 2004). In addition to its role in early stages of autophagosome formation, Atg12 has a rather uncharacteristic yet important role where it binds to Atg3 to regulate mitochondrial homeostasis during cell death (Radoshevich *et al.*, 2010). Such new functions evolve with increased complexity of eukaryotic biological systems. Core Atgs including Atg5 exhibit a high degree of conservation, however, a few proteins like Atg8,

Abbreviations used in this paper: A, adenine; aa, amino acid; Atg, autophagy; bp, base pair; BLAST, basic local alignment search tool; kDa, kilodalton; MEGA, molecular evolutionary genetic analysis; PDB, protein data bank; Pfam, protein family; Ubl, ubiquitin-like.

***Address correspondence to:** Surendra Ghaskadbi and Bhupendra Shravage. Developmental Biology Group, MACS-Agharkar Research Institute, G.G. Agarkar Road, Pune-411 004, India. Tel: +91 20 25325063. Fax: +91 20 25651542. E-mails: smghaskadbi@aripune.org; bvshravage@aripune.org
http://orcid.org/0000-0002-7367-2049 (Ghaskadbi) and http://orcid.org/0000-0002-1329-8884 (Shravage).

Supplementary Material (one table) for this paper is available at: http://dx.doi.org/10.1387/ijdb.160461sg

Submitted: 30 December, 2016; *Accepted:* 8 May, 2017; *Edited by:* Brigitte Galliot.

ISSN: Online 1696-3547, Print 0214-6282

Atg12 or Atg19 are not present in lower eukaryotes including *Eecephalitozoon cuniculi* (an intracellular fungal parasite), *Cyanidioschyzon merolae* (a unicellular haploid alga) and *Giardia intestinalis* (a protozoan parasite) (Yang *et al*., 2016). Recent studies have also revealed the emerging roles of autophagy in a variety of processes like mitochondrial homeostasis, resistance against viruses and bacteria, regeneration, tumorigenesis and apoptosis (Choi *et al*., 2013).

The cnidarian hydra has a simple body plan with two germ layers; ectoderm and endoderm and is a classic non-bilaterian model extensively used to study evolutionary developmental biology. It is also studied to understand injury-induced regeneration as it exhibits spectacular ability of regenerating lost body parts (Bode, 2003). It possesses a very simple nervous system in the form of a nerve net that allows active feeding. It usually reproduces by budding, an asexual method of reproduction. Several reports have described autophagy and its role in physiology in Hydra. For instance, Chera *et al.,* have demonstrated that Kazal-1*,* a serine protease inhibitor*,* appears to directly or indirectly regulate autophagy induction. For instance, silencing of *Kazal-1* induces autophagy in gland cells and digestive (endodermal myoepithelial cells) (Chera *et al*., 2006). In another study, autophagy was monitored using markers such as Atg8/LC3 and LysoTracker in response to rapamycin, wortmannin and BafilomycinA1 in Hydra (Buzgariu *et al*., 2008). The conservation of autophagy pathway in Hydra was shown in prolonged starvation studies which induced autophagy in both ectodermal and endodermal cells (Chera *et al*., 2009). Using RNA-seq techniques, several Atgs were shown to be expressed in purified ectodermal as well as endodermal cells (Buzgariu *et al*., 2015). Although these studies demonstrate presence of Atgs and induction of autophagy in Hydra, in-depth analyses and expression studies of Hydra Atgs are lacking. Characterizing autophagy related genes in hydra will aid in understanding their evolution. In addition, studies of autophagy related genes and their phylogenetic relation with orthologs amongst eukaryotes may illuminate the evolutionary aspects of the autophagy network and the diversification of their functions in different taxa.

Here we present identification and characterization of *Atg12* and *Atg5* from *Hydra vulgaris* Ind Pune. Bioinformatics and phylogenetic analyses demonstrate the conserved nature of these proteins at the sequence as well as structural levels. Whole mount *in situ* hybridization revealed expression of *Atg12* very high in nematoblasts while *Atg5* was found to be expressed ubiquitously in the body column with higher levels of expression in budding region and growing buds of hydra polyps.

Results and Discussion

HyAtg12 shows higher identity with vertebrate Atg12 at the amino acid level

tBlastX of zebrafish *Atg12* complete coding sequence in *Hydra magnipapillata* genome resulted in identification of putative 372 bp sequence for *Atg12*. The sequence was amplified, cloned, sequenced and has been deposited in NCBI database with accession number KT071608.1. Hereafter, *Atg12* gene from hydra will be termed as *HyAtg12*. Consistent with the fact that hydra genome is A+T rich; *HyAtg12* contained 66.4% of A+T content. The predicted amino acid sequence is 123 aa for Atg12 with approximate molecular weight of 13 kDa (Fig. 1A and B; Gasteiger *et al*., 2003). HyAtg12 protein sequence was compared with non-vertebrate and vertebrate orthologs using multiple sequence

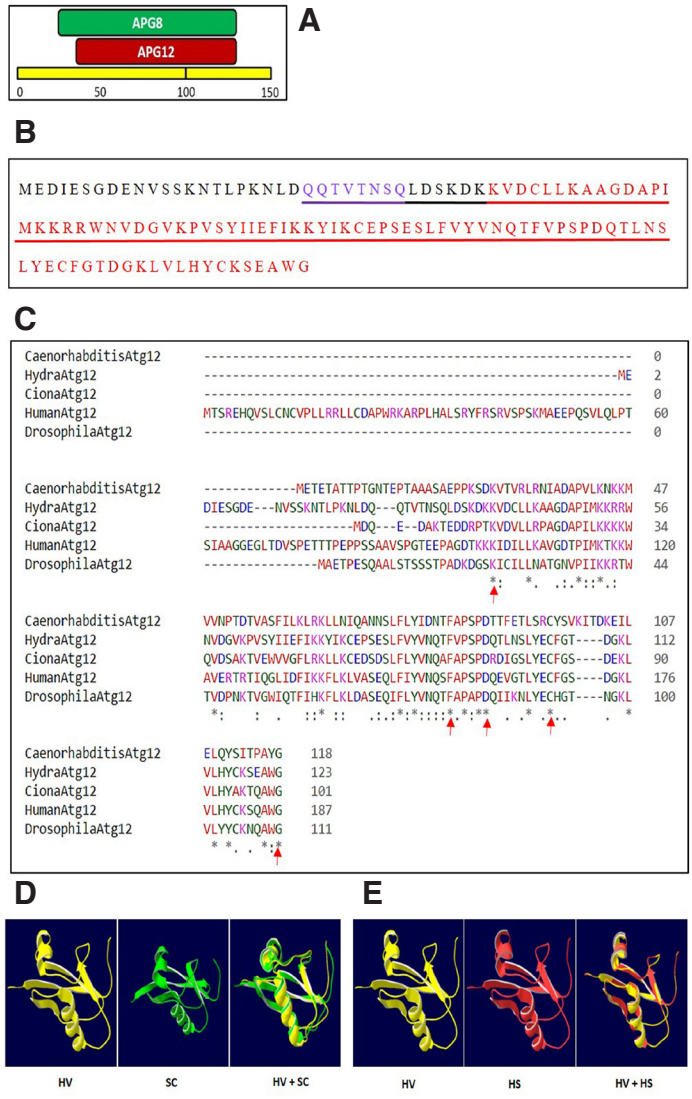

Fig. 1. SMART analyses, Pfam domain, multiple sequence alignments and homology modelling of HyAtg12. (A) *SMART analyses of HyAtg12 protein show characteristic APG12 domain.* **(B)** *Amino acid sequence of HyAtg12 underlined to show Pfam regions. Part underlined with purple indicates Atg8 Pfam region which overlaps with APG12 region colored with red.* **(C)** *MSA of complete HyAtg12 protein with corresponding animal orthologs show conservation of amino acid residues. Arrows indicate important residues for Atg12-Atg5 interactions and complex formation. (*) indicates position with single fully conserved residue, (:) indicates conservation between groups of strongly similar properties and (.) indicates conservation between groups of weakly similar properties.* **(D,E)** *Tertiary structures of Atg12 of hydra, human and yeast were simulated from available solved structures using Swiss Model Tool.* **(D)** *HyAtg12 and yeast Atg12 were superimposed using Iterative Magic Fit tool in SPDBV (RMSD: 1.08A°)* **(E)** *HyAtg12 and Human Atg12 superimposed using Iterative Magic Fit tool in SPDBV (RMSD: 0.09A°) HV:* Hydra vulgaris, *SC:* Saccharomyces cerevisiae, *HS:* Homo sapiens. *Accession numbers of the sequences used for MSA: Human (AAH12266.2),* Drosophila *(NP 648551.3),* Ciona *(XP 004226941.1), and* Caenorhabditis *(NP 498228.1).*

alignment (MSA) function in Clustal Omega (Fig. 1C; and Sievers and Higgins, 2014). HyAtg12 showed maximum percent identity of 56.44% with Atg12 of *Ciona* followed by human Atg12 showing identity of 51.22% (Supplementary Table S1A).

HyAtg12 possesses APG12, a ubiquitin-like domain

Simple Modular Architecture Research Tool (SMART) analysis of HyAtg12 protein sequence revealed characteristic functional Pfam region APG12. APG12 domain spans from 37 to 123 amino acids of HyAtg12 in *H. vulgaris* Ind Pune (Fig. 1B). HyAtg12 was also found to contain Atg8 Pfam region spanning from 23 to 123 amino acids (Fig. 1B). This was expected as both Atg12 and Atg8 belong to the ubiquitin-like superfamily of proteins. The MSA of HyAtg12 with other animals revealed several amino acid residues conserved in Atg12 (Fig. 1C). Previous studies of human (Hs) and yeast (Sc) Atg12 have shown that these conserved amino acid residues are crucial for the formation and stability of Atg12-Atg5 complex. For instance, the terminal glycine (G) residue conserved at position 187 in HsAtg12 is found at position 123 in HyAtg12 (Fig. 1C, marked with an arrow). Atg12-Atg5-Ag16 complex has been shown to function as E3 like-ligase, regulating the lipidation of Atg8/LC3 (Walczak and Martens, 2013). Several residues have been shown to be important for the E3 activity of Atg12-Atg5-Atg16 complex. For example, mutations in conserved Asp160 and Cys169 of human Atg12 (Asp96 and Cys105 in HyAtg12) (Fig. 1C, marked with arrows) severely compromise the E3 activity of the Atg12-Atg5-Atg16 complex both *in vitro* and *in vivo* (Otomo *et al*., 2013).

Atg12-Atg5 is processed by Atg3, an E2-like enzyme, to generate Atg12-Atg5-Atg16 complex (Matsushita *et al*., 2007). The interaction with Atg3 is mediated by two lysine residues present at position 101 and 119 in HsAtg12. K101 of HsAtg12 is conserved in HyAtg12 present at position 37 (Fig. 1C, marked with an arrow). Atg12 can form a complex with Atg3 under certain nutrient limiting conditions where the complex is known to play an important role in maintaining mitochondrial homeostasis and preventing cell death (Radoshevich *et al*., 2010).

Predicted structures of HyAtg12 show similarity with solved structures from other animals

Crystal structure of Atg12-Atg5 conjugate from both yeast and humans have been solved and are deposited as 3W1S, 4GDK and 4GDL and have a resolution of 2.0°A or better (Suzuki *et al*., 2016). Amino acid sequence of HyAtg12 was used as query to search templates showing similarity in Swiss-Model Program (Guex and Peitsch, 1997). The analysis showed HsAtg12 (4GDK) as the first hit indicating close similarity between hydra and human Atg12. The simulated HyAtg12 protein structure showed two α helices and four β pleated sheets (Fig. 1D). We compared 3D protein structures of HyAtg12, HsAtg12 and ScAtg12 to get a greater insight into the degree of similarity at the structural level. RMSD value of superimposed structures for HyAtg12 and ScAtg12 was 1.08A° and for HyAtg12 and HsAtg12 was 0.09A°, suggesting high degree of similarity between HyAtg12 and human, as well as yeast Atg12 (Fig. 1 D,E). Taken together, this suggests that Atg12 structure has remained conserved and largely unchanged due to strong evolutionary pressure given the critical role of Atg12 during early stages of autophagosome formation.

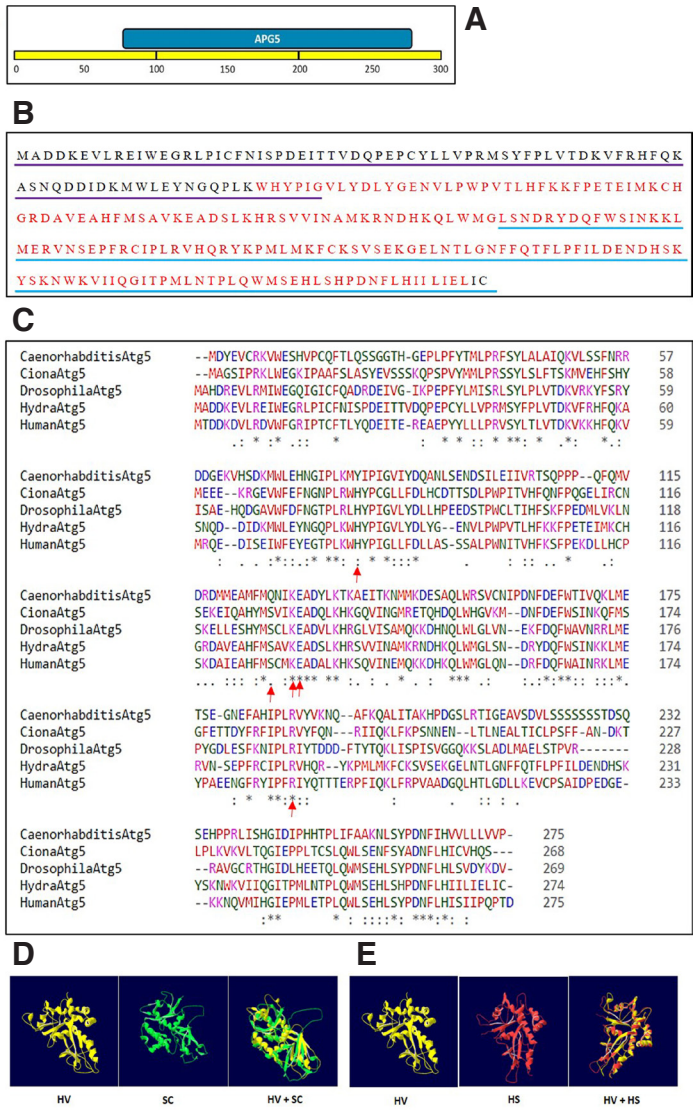

Fig. 2. SMART analyses, Pfam domain, multiple sequence alignments and homology modelling of HyAtg5. (A) *SMART analyses of HyAtg5 protein show characteristic APG5 domain.* **(B)** *Amino acid sequence of HyAtg5 highlighted to show Pfam regions. Part underlined with purple depicts UblA region of HyAtg5 and part underlined with blue indicates UblB region of HyAtg5. Region colored in red is APG5 Pfam.* **(C)** *MSA of complete HyAtg5 protein with corresponding animal orthologs show conservation of amino acid residues. Arrows indicate important residues for Atg12-Atg5 interactions and complex formation. (*) indicates position with single fully conserved residue, (:) indicates conservation between groups of strongly similar properties and (.) indicates conservation between groups of weakly similar properties.* **(D,E)** *Tertiary structures of Atg5 of hydra, human and yeast were simulated from available solved structures using Swiss Model Tool.* **(D)** *HyAtg5 and yeast Atg5 superimposed using Iterative Magic Fit tool in SPDBV (RMSD: 1.39A°)* **(E)** *HyAtg5 and Human Atg5 superimposed using Iterative Magic Fit tool in SPDBV (RMSD: 0.42A°). HV:* Hydra vulgaris, *SC:* Saccharomyces cerevisiae, *HS:* Homo sapiens. *Accession numbers of the sequences used for MSA: Human (AGC52703.1),* Drosophila *(NP 572390.1),* Ciona *(NP 001071885.1), and* Caenorhabditis *(NP 490885.3).*

HyAtg5 shows higher identity with vertebrate Atg5 at the amino acid level

tBlastX of zebrafish *Atg5* complete coding sequence in *Hydra magnipapillata* genome resulted in identification of putative 825 bp sequence for *Atg5*. The sequence was amplified, cloned, sequenced and has been deposited in NCBI database with accession number KT071609.1. Henceforth, *Atg5* gene from hydra will be termed as *HyAtg5*. *HyAtg5* is AT rich and has 65.6% of A+T content. The predicted amino acid sequence is 274 aa for Atg5 in length and its approximate molecular weight is 32-kDa (Fig. 2A and B; Gasteiger *et al.*, 2003). Using multiple sequence alignment (MSA) function in Clustal Omega HyAtg5 protein sequence was compared with non-vertebrate and vertebrate orthologs (Fig. 2C; Sievers and Higgins, 2014). HyAtg5 showed maximum identity of 55.93% with human Atg5 followed by *Drosophila* (45.25%). (Supplementary Table S1B).

HyAtg5 bears an APG5 domain

SMART analysis of HyAtg5 protein sequence revealed characteristic functional Pfam domain APG5. APG5 stretches from amino acids 80 to 272 of HyAtg5 (Fig. 2B). Atg5 belongs to the Ubiquitin-like (Ubl) family of proteins and comprises Ubl-like domains at the N- and C-terminal termed as UblA (Fig. 2B; underlined in purple) and UblB (Fig. 2B; underlined in blue), and separated by helix-rich domain. The MSA of HyAtg5 with other animals revealed several amino acid residues conserved in Atg5 (Fig. 2C). The terminal glycine (G) residue of HsAtg12 participates in formation of covalent bond with lysine (K) 130 of HsAtg5 and is necessary for covalent bond formation in the Atg12-Atg5 complex (Otomo *et al.*, 2013). This critical lysine residue of Atg5 is present at position 130 in HyAtg5 (Fig. 2C, marked with an arrow). Many such residues important in Atg12-Atg5 interaction are found to be conserved in human (Fig. 2C). Mutations in His80, Ser127 of human Atg5 (His81 and Ser127in HyAtg5) (Fig. 2C, marked with arrows) adversely affect the E3 activity of the Atg12-Atg5-Atg16 complex (Otomo *et al.*, 2013). This high level of conservation of amino acid residues observed at the interface is indicative of strong evolutionary pressure on the Atg12-Atg5 architecture. Thus, HyAtg12 and HyAtg5 possess conserved domains and the critical amino acids residues that are necessary for the proper interaction with other autophagy related proteins.

Predicted structures of HyAtg5 show similarity with solved structures of other animals

The simulated HyAtg5 structure showed nine α helices and ten β pleated sheets (Fig. 2D). In case of Atg5, RMSD value of HyAtg5 and ScAtg5 superimposed was 1.39A° and, for HyAtg5 and HsAtg5, it was 0.42A° (Fig. 2 D,E). RMSD value less than 2A° indicates higher identity between amino acid sequences of HyAtg12 and HyAtg5 with their respective orthologs in human and yeast (Guex and Peitsch, 1997). In summary, Atg12 and Atg5 are conserved across species at the sequence as well as structural level.

HyAtg12 *clusters with non-vertebrate counterparts in phylogenetic analysis*

To get a deeper insight into the evolutionary relationships amongst *Atg12* and *Atg5* genes we subjected these two genes to phylogenetic analyses using Mr. Bayes. Phylogenetic analysis for *HyAtg12* is discussed here (Fig. 3). The value at each branch of the tree depicts the probability of replicates in which the associated taxa arise from the same point. *Saccharomyces* was selected as outgroup and served as a root in both *Atg12* and *Atg5* phylogenetic analyses. Since we were interested in statistically supported part of tree where hydra gets grouped with major clade, analysis was

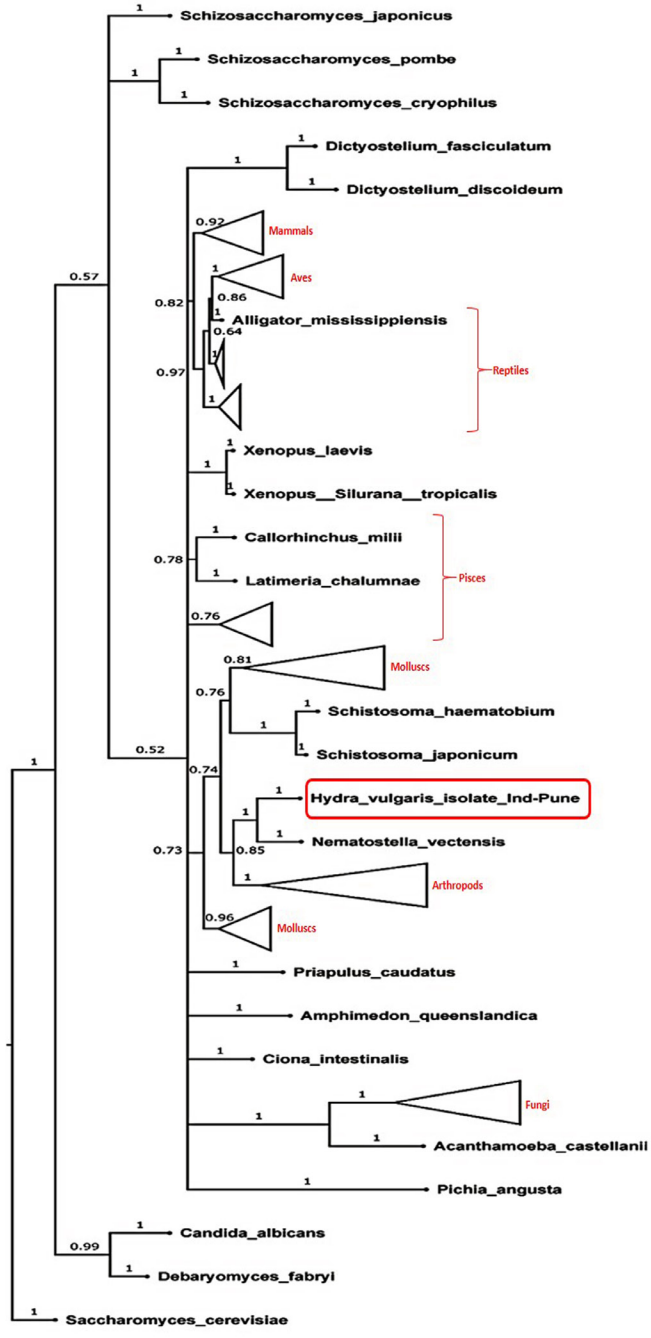

Fig. 3. Phylogenetic analysis of HyAtg12. *Phylogenetic tree for* Atg12 *was obtained by Bayesian Method and visualized using FigTree 1.4.3. Branch values are probabilities of the branches to emerge from the same point after every generation during analysis. Branch values have been shifted near respective branches for reading purpose.* Saccharomyces *served as a root while building trees.* HyAtg12 *grouped with other Cnidarians and later with arthropods and molluscs to form a major clade indicating the closeness with non-vertebrates.*

stopped after standard deviation of split frequencies was 0.05 (Ronquist *et al*., 2012). Probability value 1 at branch point indicates 100% of the taxa arise from same point. *HyAtg12* formed immediate group with *Nematostella Atg12*, member of the phylum Cnidaria. This group was found to cluster with a major clade of arthropods and later with molluscs and Platyhelminthes (e.g. *Schistosoma*). This indicates phylogenetic closeness of hydra *Atg12* with non-vertebrates (Fig. 3).

HyAtg5 *clusters with non-vertebrates in phylogenetic analysis*

We performed a similar Bayesian analyses for *HyAtg5*. Although the branching pattern differed amongst *Atg5* sequences the phylogenetic relationships at the phylum level remained similar as observed in case of *HyAtg12*. The analyses revealed that *HyAtg5* clubbed with a small clade of *Nematostella* and *Acropora*, animals belonging to the same phylum Cnidaria. This clade of cnidarians showed closeness with other non-vertebrates like molluscs (Fig. 4). Thus, both *HyAtg12* and *HyAtg5* showed phylogenetic closeness with non-vertebrates.

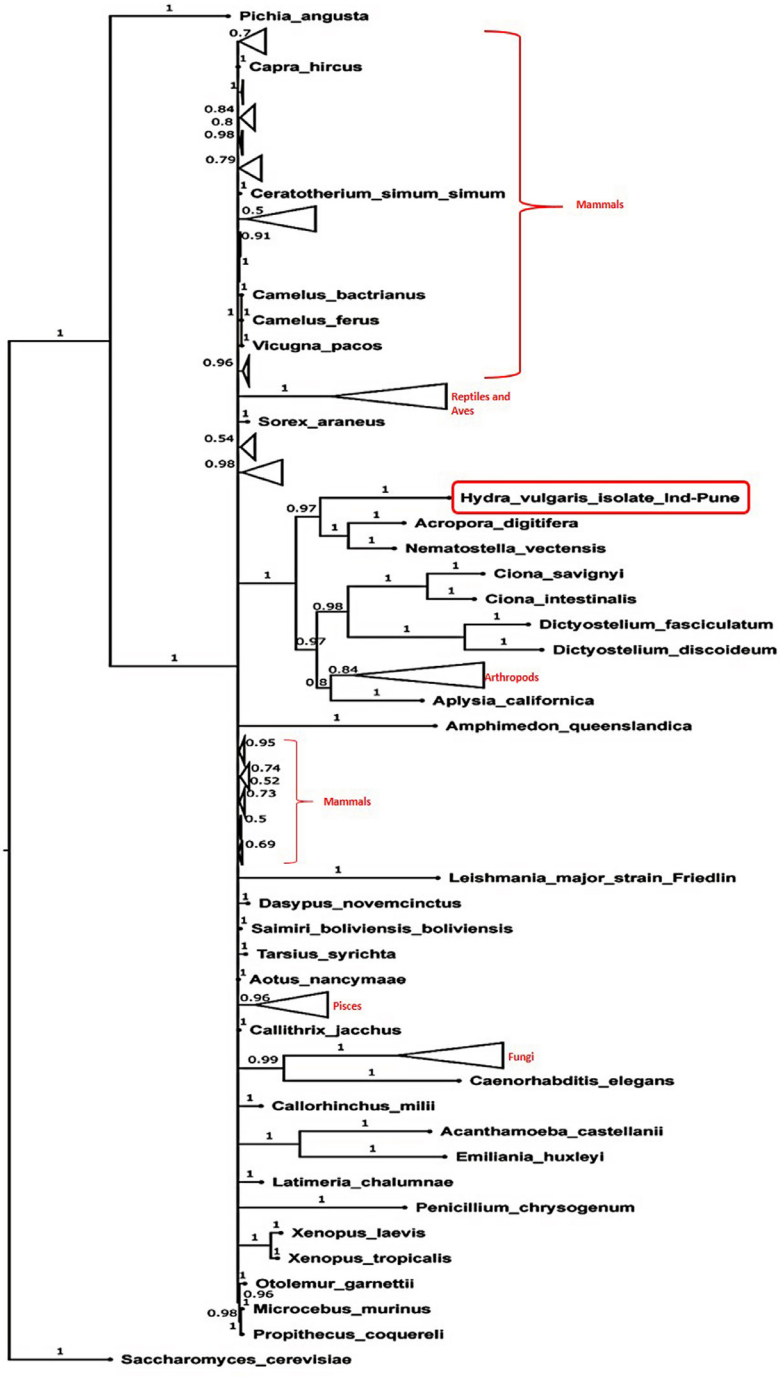

HyAtg12 *and* HyAtg5 *transcripts are expressed in the body column of hydra*

Whole mount *in situ* hybridization was carried out for localization of *HyAtg12* and *HyAtg5* transcripts in whole polyps. *Atg12* transcripts were detected in groups of cells in the entire body column of the polyp and the growing buds (Fig. 5 B,F). *Atg12* expression was found to be excluded from the head, tentacles and foot region (Fig. 5 B,C-F). When observed at higher magnification *Atg12* was found to be expressed in 6-8, 8-16 cell clusters present in the ectoderm which resemble nematoblasts (Fig.5G and Shimizu and Bode, 1995). Nematoblasts are derived from interstitial cells (I-cells) found in clusters of 6-8 cells, and later differentiate into nematocytes, which are essential for capture of prey (Shimizu and Bode, 1995). HyAtg12 expression is not restricted to ectodermal nematoblasts but also found in at low levels in both ectodermal and endodermal epithelial cells (Fig. 5 H,I). This suggests that *HyAtg12* may have a crucial role in specification and/or maintenance of nematoblasts. Recently, it was reported that several Atgs including *Atg12* are expressed at a uniform low level in ectodermal, endodermal and interstitial stem cells (Buzgariu *et al*., 2015). While *Atg5* transcripts were also found to be expressed primarily in the body column, unlike Atg12, their expression did not appear to be restricted to specific cells or groups of cells (Fig. 5 K,L). *Atg5* transcripts were excluded from the hypostome as well as the foot region. (Fig. 5 M-P). In budding polyps *Atg5* transcripts were found to be concentrated in the budding region and the growing bud of the polyp (Fig. 5 Q,R). This may indicate role of *Atg5* in initiation of budding and growth of buds in hydra. To rule out asymmetry of expression within the ectoderm and the endoderm, we imaged *Atg5* hydra polyps at a high magnification. An optical longitudinal section showed no difference in the intensity of staining across the endodermal and ectodermal region in the body column (Fig. 5 S,T).

The present study shows that hydra possesses the core autophagy genes, *Atg12* and *Atg5*. Domain and Pfam analyses hint at the highly-conserved nature of these genes at the domain level. Multiple sequence alignment showed significant degree of conservation of amino acids important for Atg12-Atg5 interaction and complex formation.

Fig. 4. Phylogenetic analysis of HyAtg5. *A phylogenetic tree for* Atg5 *was obtained by Bayesian Method and visualized using FigTree 1.4.3. Branch values are probabilities of the branches to emerge from the same point after every generation during analysis. Branch values have been shifted near respective branches for reading purpose.* Saccharomyces *served as a root while building trees.* HyAtg5 *grouped with other Cnidarians and further with arthropods to form a single clade indicating their closeness with non-vertebrates.*

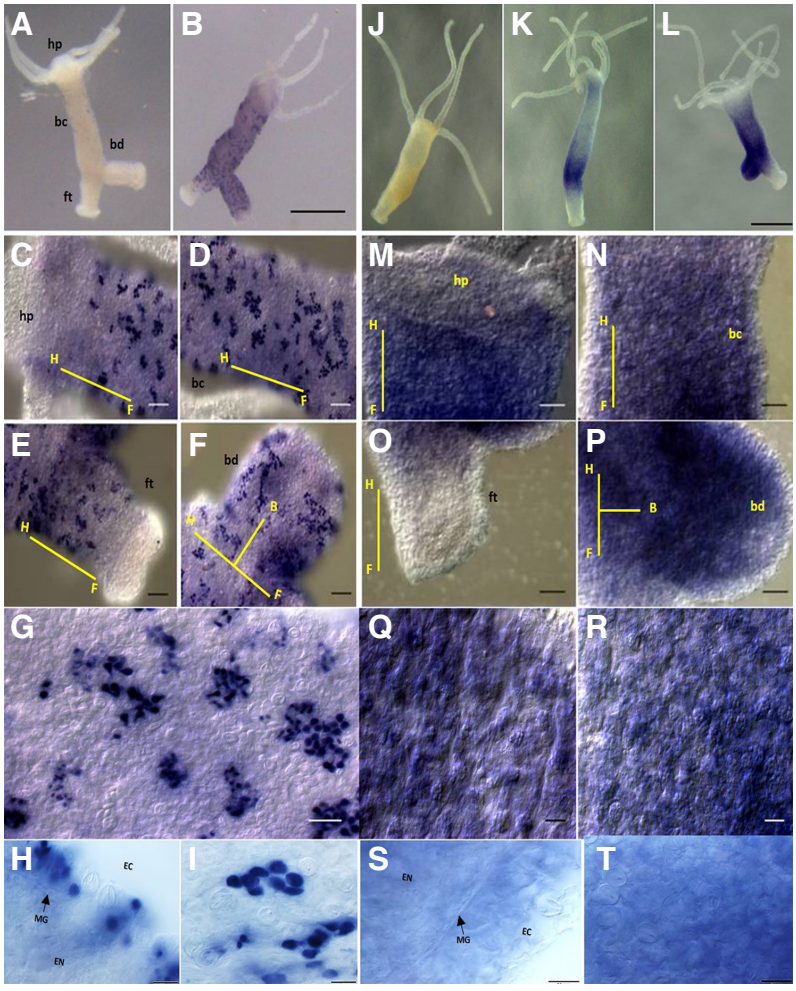

Fig. 5. Localization of HyAtg12 and HyAtg5 transcripts. *Transcripts of* Atg12 *and* Atg5 *were localized by whole mount* in situ *hybridization.* **(A)** *Whole mount* in situ *hybridization with* Atg12 *sense riboprobe.* **(B)** *Shows expression of* Atg12 *in whole polyp.* **(C-F)** *Expression of* Atg12 *transcripts in hypostomal region, body column, foot region and bud of hydra, respectively.* **(G)** *Expression of* Atg12 *in clusters of nematoblasts and in epithelial cells of ectoderm of body column.* **(H,I)** *Show profound expression of* Atg12 *in ectodermal nematoblasts cells and lower level of expression in endodermal epithelial cells.* **(J)** *Whole mount* in situ *hybridization with* Atg5 *sense riboprobe.* **(K)** *Expression of* Atg5 *in body column in of non-budding polyp and* **(L)** *in budding polyp and the growing bud.* **(M-P)** *Magnified view of L to show expression of* Atg5 *in hypostomal region, body column, foot region and bud of hydra, respectively.* **(Q)** *Prominent expression of* Atg5 *in budding region of hydra polyp shown in K and* **(R)** *in growing bud shown in L.* **(S,T)** *Show expression of* Atg5 *in both ectodermal and endodermal cells. hp: hypostome, bc: body column, ft: foot region, bd: bud. Scale bars: (A,B,J,K,L) 200 μm; (C,D,E,F and M,N,O,P) 50 μm; (G,Q,R) 20 μm; (H,I,S,T) 10 μm. Orientation of animal is indicated with line drawings in yellow in (C,D,E,F and M,N,O,P). H, head; F, foot; B, bud; EC, ectoderm; EN, endoderm; MG, mesoglea.*

Homology modelling suggests that HyAtg12 and HyAtg5 protein structures are highly similar to their human counterparts. *HyAtg12* and *HyAtg5* showed closeness with non-vertebrate orthologs in Bayesian phylogenetic analyses. In addition, both these genes showed similarity with respective orthologs in yeast indicating early origin of these genes in eukaryotes. Localization of *HyAtg12* and *HyAtg5* transcripts using *in situ* hybridization showed their predominant expression in body column of polyps. *Atg12* transcripts were found to be expressed in 6-8 or larger cell clusters in the ectoderm with relatively low level expression in all endodermal cells. The cell clusters resemble nematoblasts and *Atg12* may have a role in their specification and/or maintenance. Expression of *Atg5* was found to be in both ectoderm and endodermal cells. Significantly higher levels of *Atg5* in budding region as well as in growing buds suggest its possible role in initiation and progression of budding. Although autophagy related genes show conservation across eukaryotes, the mechanism of autophagy varies across different taxa depending on a multitude of factors as well as complexity of organisms. Hydra is an early-branched metazoan and given its position in the tree of life, it may serve as a useful model to study the evolution of the autophagy network. In addition, the specific expression of these two autophagy genes indicates a crucial role of autophagy in various developmental and physiological processes in hydra.

Materials and Methods

Culture and maintenance of hydra

Polyps of *H. vulgaris* Ind Pune (Reddy *et al.*, 2011) were maintained at 18°C with a 12 hour day and night cycle. Hydra were kept in a medium containing KCl (0.1 mM), NaCl (1 mM), $MgSO_4.7H_2O$ (0.1 mM), $CaCl_2.2H_2O$ (1 mM) and Tris base (1 mM) (Bossert and Galliot, 2012). Hydra were fed with freshly hatched nauplii of the crustacean *Artemia salina.*

Amplification and cloning of Atg12 *and* Atg5

Following primers were used for amplification of *Atg12* sense primer 5'-ATGGAAGATATTGAATCAGGAGATGAAAAC and antisense primer 5'-TTAACCCCAAGCCTCAGATTTGC and for *Atg5* sense primer 5'-ATGGCAGACGACAAGGAGGT and antisense primer 5'-CTAACATATCAATTCAATCAAAATAATATGCAG. Total RNA was extracted from hydra using TriReagent (Sigma, USA). cDNA was synthesized using Verso cDNA synthesis kit according to manufacturer's instructions (Thermo Fisher Scientific, USA). Putative *Atg12* and *Atg5* sequences were amplified and cloned in pGEM-T Easy Vector (Promega, USA). The cloned inserts were sequenced using Sanger's DNA sequencing method (1st Base, Malaysia).

Conserved domain analysis and multiple sequence alignment

Putative HyAtg12 and HyAtg5 were analysed for their characteristic functional domains using Simple Modular Architecture Research Tool (SMART) (Gasteiger, 2003; Letunic *et al.*, 2015). HyAtg12 and HyAtg5 were compared with their human, *C. elegans*, *Ciona*, and *Drosophila* counterparts using multiple sequence alignment in Clustal Omega for determining identity among the sequences (Sievers and Higgins, 2014).

Homology modelling

Homology modelling was carried out to understand tertiary structures for putative HyAtg12 and HyAtg5 using Swiss Model program at ExPaSy Server (Biasini *et al.*, 2014). The generated models were compared with solved models of yeast and human for homology using Swiss PDB Viewer Software Deep View (Guex and Peitsch, 1997). Superimposition of models was carried out using Iterative Magic Fit and degree of similarity between the models was assessed from Root Mean Square Deviation (RMSD) values for superimposed peptides.

Phylogenetic analysis

Phylogenetic analyses of *Atg12* and *Atg5* from various species was performed using Bayesian method (Ronquist *et al*., 2012). The sequences were aligned using ClustalX 2.1 (Larkin *et al*., 2007) and the alignments were used to build phylogenetic trees in Mr. Bayes. In Mr. Bayes, evolutionary model was set to General Time Reversible (GTR) substitution with gamma distributed rate variation across the sites and proportion of invariable sites. With posterior probability distribution, diagnostics were calculated per 1, 00,000 generations. Chain length was kept 4 so that three heated chains and one cold chain will be used in Metropolis coupling to improve MCMC sampling of target distribution. Melting temperature was set to 0.5°C considering the acceptance rate of chains. Lower temperature was set to facilitate swapping of heated and cold chains states. The analysis was run till average standard deviation of split frequencies was equal to or below 0.05. Burn in was 25% of total generations. The phylogenetic trees were visualized using FigTree version 1.4.3.

Whole mount* in situ *hybridization

Whole mount *in situ* hybridization was carried out to localize transcripts of *Atg12* and *Atg5* as described by (Krishnapati and Ghaskadbi, 2013) with a few modifications. Hydra were starved for 48hr. They were relaxed in 2% urethane for 90 seconds and later fixed in 4% paraformaldehyde (PFA) overnight at 4°C. DIG-labelled, single-stranded RNA probes (sense and antisense) were generated by *in vitro* transcription (Roche). Hybridization with DIG-labeled probes was carried out for ~60 h at 60°C. The reaction was detected by alkaline phosphatase staining with nitro blue tetrazolium (NBT) and 5-bromo-4-chloro-3-indolyl-phosphate p-toluidine salt (BCIP) system.

Acknowledgements

We thank Dr. Vidya Patwardhan, Dr. K.L. Surekha and other members of the lab for discussions, Dr. Ritesh Kumar Choudhary for his help with phylogenetic analyses. IISER, Pune and Dr. Karthick Balasubramanian for providing access to DIC microscopy facilities. ND is supported by a Senior Research Fellowship from Indian Council of Medical Research (ICMR), New Delhi. This work was supported by intramural grants from MACS-Agharkar Research Institute, Pune (Project Zoo-17) and Emeritus Scientist scheme from Council for Scientific and Industrial Research (CSIR), New Delhi to SG.

References

BIASINI M, BIENERT S, WATERHOUSE A, ARNOLD K, STUDER G, SCHMIDT T, KIEFER F, CASSARINO TG *et al.,* (2014). SWISS-MODEL: Modelling protein tertiary and quaternary structure using evolutionary information. *Nucleic Acids Res* 42: W252–W258.

BODE H (2003). Head regeneration in hydra. *Dev Dyn* 226: 225-236.

BOSSERT P, GALLIOT B (2012). How to use Hydra as a model system to teach biology in the classroom. *Int J Dev Biol* 56: 637–652.

BUZGARIU W, CHERA S, GALLIOT B (2008) Methods to investigate autophagy during starvation and regeneration in hydra. *Methods Enzymol* 451: 409-437

BUZGARIU W, A HADDAD S, TOMCZYK S, WENGER Y, GALLIOT B (2015) Multifunctionality and plasticity characterize epithelial cells in Hydra. *Tissue Barriers* 3: e1068908.

CHERA S., R. DE ROSA, M. MILJKOVIC-LICINA, K. DOBRETZ, L. GHILA, K. KALOULIS, B. GALLIOT (2006) Silencing of the hydra serine protease inhibitor *Kazal1* gene mimics the human SPINK1 pancreatic phenotype. *J Cell Sci* 119: 846–857.

CHERA S, BUZGARIU W, GHILA L, GALLIOT B (2009). Autophagy in Hydra: A response to starvation and stress in early animal evolution. *Biochim Biophys Acta - Mol Cell Res* 1793: 1432–1443.

CHOI AMK, RYTER SW, LEVINE B (2013). Autophagy in Human Health and Disease. *N Engl J Med* 368: 651–662.

GASTEIGER E, GATTIKER A, HOOGLAND C, IVANYI I, APPEL RD, BAIROCH A (2003). ExPaSy: The proteomics server for in-depth protein knowledge and analysis. *Nucleic Acids Res* 31: 3784–3788.

GUEX N, PEITSCH MC (1997). SWISS-MODEL and the Swiss-Pdb Viewer: An environment for comparative protein modeling. *Electrophoresis* 18: 2714–2723.

KRISHNAPATI, L.S., GHASKADBI, S. (2013). Identification and characterization of VEGF and FGF from Hydra. *Int J Dev Biol* 57: 897-906.

KUMA A, HATANO M, MATSUI M., YAMAMOTO A, NAKAYA H, YOSHIMORI T, OHSUMI Y, TOKUHISA T, *et al.,* (2004). The role of autophagy during the early neonatal starvation period. *Nature* 432: 1032–1036.

LARKIN MA, BLACKSHIELDS G, BROWN NP, CHENNA R, MCGETTIGAN PA, MCWILLIAM H, VALENTIN F, WALLACE IM, *et al.,* (2007). Clustal W and Clustal X version 2.0. *Bioinformatics* 23: 2947–2948.

LETUNIC I, DOERKS T, BORK P (2015). SMART: Recent updates, new developments and status in 2015. *Nucleic Acids Res* 43: D257–D260.

MATSUSHITA M, SUZUKI NN, OBARA K, FUJIOKA Y, OHSUMI Y, INAGAKI F (2007). Structure of Atg5-Atg16, a complex essential for autophagy. *J Biol Chem* 282: 6763–6772.

OHSUMI Y, MIZUSHIMA N. (2004). Two ubiquitin-like conjugation systems essential for autophagy. *Semin Cell Dev Biol* 15: 231-236.

OTOMO C, METLAGEL Z, TAKAESU G, OTOMO T (2013). Structure of the human ATG12~ATG5 conjugate required for LC3 lipidation in autophagy. *Nat Struct Mol Biol* 20: 59–66.

RADOSHEVICH L, MURROW L, CHEN N, FERNANDEZ E, ROY S, FUNG C, DEBNATH J (2010). ATG12 conjugation to ATG3 regulates mitochondrial homeostasis and cell death. *Cell* 142: 590–600.

REDDY P, BIDAYE S, GHASKADBI S (2011). Genome-wide screening reveals the emergence and divergence of RTK homologues in basal Metazoan *Hydra magnipappilata. J Biosci* 36: 289-296.

RONQUIST F, TESLENKO M, VAN DER MARK P, AYRES DL, DARLING A, HÖHNA S, LARGET B, LIU L, *et al.,* (2012). Mr. Bayes 3.2: efficient Bayesian phylogenetic inference and model choice across a large model space. *Syst Biol* 61: 539-542.

SHIMIZU H, BODE HR (1995). Nematocyte differentiation in hydra: commitment to nematocyte type occurs at the beginning of the pathway. *Dev Biol* 169: 136-150.

SIEVERS F, HIGGINS DG (2014). Clustal omega, accurate alignment of very large numbers of sequences. *Methods Mol Biol* 1079: 105–116.

SUZUKI H, OSAWA T, FUJIOKA Y, NODA NN (2016). Structural biology of the core autophagy machinery. *Curr Opin Struct Biol* 43: 10-17.

TSUKADA, M., OHSUMI, Y. (1993). Isolation and characterization of autophagy-defective mutants of Saccharomyces cerevisiae. *FEBS Lett* 333: 169–174.

WALCZAK M, MARTENS S (2013). Dissecting the role of the Atg12-Atg5-Atg16 complex during autophagosome formation. *Autophagy* 9: 424–425.

YANG J, CHAI XQ, ZHAO XX, LI X (2016). Comparative genomics revealed the origin and evolution of autophagy pathway. *Jnl of Sytematics Evolution* 55: 71-82.

Further Related Reading, published previously in the *Int. J. Dev. Biol.*

UV induced foot duplication in regenerating hydra is mediated by metalloproteinases and modulation of the Wnt pathway
Lakshmi-Surekha Krishnapati, Rohini Londhe, Vaishali Deoli, Apurva Barve, Saroj Ghaskadbi and Surendra Ghaskadbi
Int. J. Dev. Biol. (2016) 60: 111-117
https://doi.org/10.1387/ijdb.130253sg

Identification and characterization of VEGF and FGF from Hydra
Lakshmi-Surekha Krishnapati and Surendra Ghaskadbi
Int. J. Dev. Biol. (2013) 57: 897-906
https://doi.org/10.1387/ijdb.130077sg

Hydra, a fruitful model system for 270 years
Brigitte Galliot
Int. J. Dev. Biol. (2012) 56: 411-423
https://doi.org/10.1387/ijdb.120086bg

The Trembley Effect or the birth of marine zoology
Marc J. Ratcliff
Int. J. Dev. Biol. (2012) 56: 425-436
https://doi.org/10.1387/ijdb.123520mr

Germline stem cells and sex determination in Hydra
Chiemi Nishimiya-Fujisawa and Satoru Kobayashi
Int. J. Dev. Biol. (2012) 56: 499-508
https://doi.org/10.1387/ijdb.123509cf

Hydra, a versatile model to study the homeostatic and developmental functions of cell death
Silke Reiter, Marco Crescenzi, Brigitte Galliot and Wanda Buzgariu
Int. J. Dev. Biol. (2012) 56: 593-604
https://doi.org/10.1387/ijdb.123499sr

Hydra, the everlasting embryo, confronts aging
Daniel E. Martínez and Diane Bridge
Int. J. Dev. Biol. (2012) 56: 479-487
https://doi.org/10.1387/ijdb.113461dm

The Hydra model - a model for what?
Alfred Gierer
Int. J. Dev. Biol. (2012) 56: 437-445
https://doi.org/10.1387/ijdb.113458ag

5 yr ISI Impact Factor (2013) = 2.879